Journal of Membrane Science and Research 2 (2016) 95-101

Journal of Membrane Science & Research

journal homepage: www.msrjournal.com

Research Paper

Photocatalysts in Polysulfone Membrane for the Removal of Humic Acid: The Effects of PVP and PVA on Membrane Morphology, Separation Performance and Catalytic Hindrance

H.K. Melvin Ng, A.H. Sabran, C.P. Leo*, A.L. Ahmad, A.Z. Abdullah

School of Chemical Engineering, Engineering Campus, Universiti Sains Malaysia, Seri Ampangan,14300 Nibong Tebal, S.P.S., Pulau Pinang, Malaysia

ARTICLE INFO

Received 2015-11-12
Revised 2015-12-16
Accepted 2015-12-29
Available online 2015-12-29

KEYWORDS

Polysulfone membrane
Photocatalyst
Humic acid

GRAPHICAL ABSTRACT

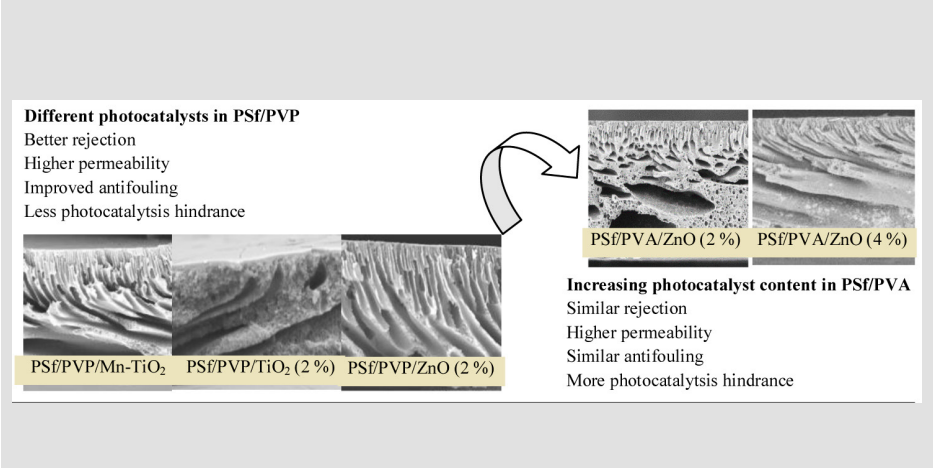

HIGHLIGHTS

- PSf/PVP with ZnO membrane rejected humic acid satisfactory
- Low hindrance of photodegradation when ZnO blended o into PSf membrane with PVP
- Formation of finger-like pores is preferable for low photocatalytic hindrance

ABSTRACT

Photocatalytic membranes exhibit great potential for water treatment since they combine the filtration and photo degradation in a single unit. Although blending photocatalytic nanoparticles into polymeric thin film remains the simplest method to prepare the photocatalytic membrane, the entrapped photocatalyst showed less catalytic activity due to the agglomeration and shielding effects in the polymer matrix. In this work, PVP (polyvinyl pyrrolidone) and PVA (poly(vinyl alcohol)) were used to stabilize the photocatalytic nanoparticles (TiO_2, Mn-TiO_2 and ZnO) in the polysulfone (PSf) membrane. Most importantly, these additives affect the formation of finger-like pores which influence the separation performance and also the hindrance of photocatalytic activities. The surface hydrophilicity of PSf/PVP/TiO_2 and PSf/PVP/Mn-TiO_2 membranes increased by 12.25° and 16.67°, respectively after adding photocatalysts. On the other hand, the PSf membrane with PVP and ZnO nanoparticles exhibited improvement in water permeability, about 7 times higher than the neat membrane. The PSf/PVP/ZnO membrane even offered higher rejection of humic acid (HA) than the PSf/PVP/TiO_2 and PSf/PVP/Mn-TiO_2 membranes. In the photo degradation test, ZnO only showed a reduction of 5.41% in its photo activity when it was blended into the PSf membrane with PVP. When PVA was used in the preparation of the PSf/PVA/ZnO membrane, the permeability improvement was greatly reduced compared to the PSf/PVP/ZnO membrane. PVA also resulted in a great hindrance to the photocatalytic activity of ZnO in the PSf membrane, more than 37%.

1. Introduction

Photocatalysts are popular due to their ability to remove contaminants under UV light even when they are used at a very low concentration [1]. One of the most commonly used photocatalysts is titanium dioxide (TiO_2), which can remove dyes and proteins in water effectively [2-3]. Besides being highly active under UV light, TiO_2 is also chemically and thermally stable, cheap, non-toxic, antimicrobial and hydrophilic [4]. To further enhance its photo-activity, the doping of TiO_2 with non-metals, noble metals or transition metals has been widely reported in the literature. TiO_2 doped with Mn was successfully designed to shift its absorption range from the UV light region

* Corresponding author at: Phone: +604-5996425, fax: +60 4 5941013
E-mail address: chcpleo@usm.my (C.P. Leo)

towards the visible light region [5]. Zinc oxide (ZnO) also shows promising photo-activity although it has a slightly larger band gap (3.3 eV), which requires higher energy to excite the electron from the valence band to conduction band [6]. It possesses similar properties to TiO_2 and they were widely used in the development of membranes for waste water treatment [7, 8].

Since photocatalysts have lots of advantages, many researches have been conducted to harness these superior properties. For example, the incorporation of a photocatalyst into the membrane resulted in a boost in the membrane performance. Kim *et al.* [9] commented that a higher water permeability and a greater rejection of humic acid (HA) could be achieved by coating TiO_2 on the polyethersulfone (PES) membrane compared to that of a neat PES membrane, causing an increase of as much as 171 % and 19 % respectively. ZnO nanoparticles were also blended into polyvinylidene difluoride (PVDF), polysulfone (PSf) and PES membranes. The water permeability of these membranes increased one to two fold, depending on the particle loading [10-12]. More polymeric membranes incorporated with photocatalysts were actually developed for fouling mitigation in the early years. Bae *et al.* [12-14] reported on several types of polymeric membranes blended with TiO_2 nanoparticles. Membrane fouling was reduced because the hydrophilic TiO_2 nanoparticles created a hydrated layer to hinder the accumulation of foulants, especially HA, on membrane surface. However, the photocatalytic activities of TiO_2 in the membrane have not been studied until recently. The accumulation of HA on a PVDF membrane doped with TiO_2 could be effectively reduced when the ultrafiltration was coupled with photocatalytic degradation [15]. The development of polymeric membranes blended with photocatalyst has been limited only by the catalyst content so far. This is because a high content of photocatalysts could cause agglomeration and pore plugging [16].

The agglomeration of inorganic fillers, especially nanoparticles in the membrane has been identified as the major challenge in the preparation of mixed matrix membranes. Strategies such as priming and in-situ synthesis of particles within the polymeric matrix have been practiced in the preparation of mixed matrix membranes for gas separation [17]. This similar practice was not required in the preparation of ultrafiltration membranes with nanoparticles, mainly because some additives such as polyvinyl alcohol (PVA), polyvinyl pyrrolidone (PVP), and polyethylene glycol (PEG) are usually blended together with photocatalysts into the polymer solutions of ultrafiltration membranes for pore formation [17]. These additives stabilize TiO_2 nanoparticles in thin films or in polymer composites to diminish the particle agglomeration [18-21].

As mentioned earlier, not much work has been reported on the photocatalytic activity of polymeric membranes blended with photocatalyst nanoparticles to the best of our knowledge. The main area of study so far has been on fouling mitigation, and the full potential of these photocatalytic membranes had not been explored. The magnificent improvement in the membrane separation performance has led to the oversight of the TiO_2 photocatalytic properties. For instance, Jun-Ke Pi *et al.* [22] only stated the improved surface wettability and antifouling property of the membrane after adding TiO_2 without studying photocatalytic degradation. On the other hand, those who work on photocatalytic degradation employ the surface coating method instead of blending [23]. Hence, the photo-activity of different photocatalysts in PSf membranes is studied in this work. The effects of PVP and PVA on the photocatalytic membranes are compared in terms of morphology and separation performance. The presence of various additives is expected to alter the exchange rate of solvents (NMP) and non-solvents differently during phase inversion [24]. The changes in the delay-mixing process can result in the variation of pore formation [25], where finger like pore structures in the membranes not only aided separation, but also improved the photocatalytic reaction of nanoparticles in the membranes.

2. Materials and methods

2.1. Materials

PSf polymers (Udel P-1700, Solvay Advanced Polymers) were used for the fabrication of membranes. The solvent, 1-methyl-2-pyrrolidinone (NMP, >99.5%) supplied by Merck, was used without further purification. The additives (PVA and PVP, Mw 10,000) and photocatalysts (ZnO, TiO_2, and Mn-doped TiO_2, <100 nm) were supplied by Sigma Aldrich. Distilled water was used in all coagulation baths.

2.2. Membrane Synthesis

The solvent, 1-methyl-2-pyrrolidinone (NMP) was heated until the solution temperature reached 40 °C [26]. Then, 2 wt.% of each photocatalyst (ZnO, TiO_2 and Mn-doped TiO_2) was dissolved slowly into the NMP under continuous agitation of 250 rpm using a stirring hotplate (WiseStir MSH-20D). The mixture was ultrasonicated using an Ultrasonic degasser (Elma S80H) for 2 hours to obtain a well-dispersed solution. The mixture was then heated with heating (WiseStir MSH-20D). A PSf membrane without any added photocatalyst was prepared as the control sample. PVP (2 wt.%) was added slowly into the solution, followed by PSf (Udel P-1700, Solvay Advanced Polymers). The weight ratio of PSf to NMP was controlled at 1:4.84. The PSf polymer solution was stirred for 4.5 hours at 75 °C and at a stirring speed of 400 rpm to form a homogeneous polymer solution. It was then cooled to 25 °C for 1 hour before ultrasonication for 30 minutes. The casting solution was then left at room temperature to release all bubbles prior to casting.

The casting process was performed using a pneumatically controlled casting machine. The solution was spread on a clean flat glass plate using a casting knife at a gap of 150 µm. The film was left for evaporation (30 s) to form a dense layer at ambient atmosphere. The prepared membrane film was then rapidly immersed in a coagulation non-solvent bath (distilled water). After primary phase separation, the membrane was stored in fresh distilled water for 24 hours to guarantee the complete phase separation and removal of the residual solvent. Then, the membrane was peeled off and rinsed with distilled water for at least 30 minutes. At the final stage, the membrane will be dried for 24 h at room temperature before characterization. The membrane consisting of PVA was synthesized by the same method, by replacing PVP with PVA. All the photocatalysts were maintained at 2 wt.% except for 1 membrane that consists of 4 wt.% ZnO (which is denoted as PSP/PVA/ZnO-4%).

2.3. Membrane characterization

The surface and cross-sectional structure of the membrane samples were examined using a field emission scanning electron microscope (FESEM, Quanta 200 FESEM, FEI). The membranes were fractured using liquid nitrogen and coated with a thin layer of gold prior to scanning. Energy dispersive X-ray (EDX) analysis was also conducted using an INCA instrument, (Oxford Instruments, England) to confirm the elements present in the membranes. Meanwhile, the changes of surface hydrophilicity were studied by measuring the water contact angle on the surface of the membrane that was dried overnight. The contact angle was measured using a Rame'-Hart model 200 standard contact angle goniometer with DROP image Standard Software. Media used for contact angle measurement were ultrapure water and air at ambient temperature (22–23 °C).

2.4. Separation test

Membrane permeability was determined using a dead-end stirred cell, Sterlitech HP4750 (Sterlitech Corporation, WA) and ultrapure water at room temperature. The dead-end filtration cell had an active membrane area of 14.6 cm^2. Permeability of the membrane was tested in the pressure range of 1 to 4 bar after compaction using nitrogen gas. In the fouling study, the aqueous solution containing 5 mg/L of HA acid at a pH of 7 was filtered at 4 bar. The rejection of HA was measured by determining the HA concentration in the permeate samples using a UV-Vis spectrophotometer (UV-Vis Cary 60).

2.5. Photocatalytic Test

Free photocatalysts were mixed into the HA solution (concentration 5mg/L, pH7) at a weight ratio of 5×10^{-6}:1. The HA degradation with the presence of UV light was studied. A control solution was tested in the dark where no UV was present. Samples were taken at an interval of 10 minutes and the concentration of HA was determined by using a UV-Vis spectrophotometer (UV-Vis Cary 60). The experiments were repeated using membranes with different photocatalysts. The membrane samples with an area of 30.19 cm^2 were used for testing, under the assumption that they contained a similar amount of photocatalysts, and did not experience loss during synthesis.

3. Results and discussion

3.1. Morphological, hydrophilic and chemical changes on membranes

The changes in membrane morphology due to the addition of PVP, PVA and photocatalysts are shown in Figures 1 and 2. All PSf membranes with PVP exhibited asymmetric structures which consisted of a thin dense layer at the top and a sub-layer with finger-like pores at the bottom. The addition of hydrophilic PVP improved the pore interconnectivity, resulting in finger-like

pores even when photocatalysts had not yet been added into the PSf/PVP membrane [27]. Matsuyama *et al.* [28] reported a similar finding that finger-like pores were formed when PVP was added into the membrane formulation. The thermodynamic instability of the membrane caused by the presence of PVP greatly promoted the growth rate of pores. The excessive formation of nuclei was inhibited and hence the formation of spongy structures was prevented [29].

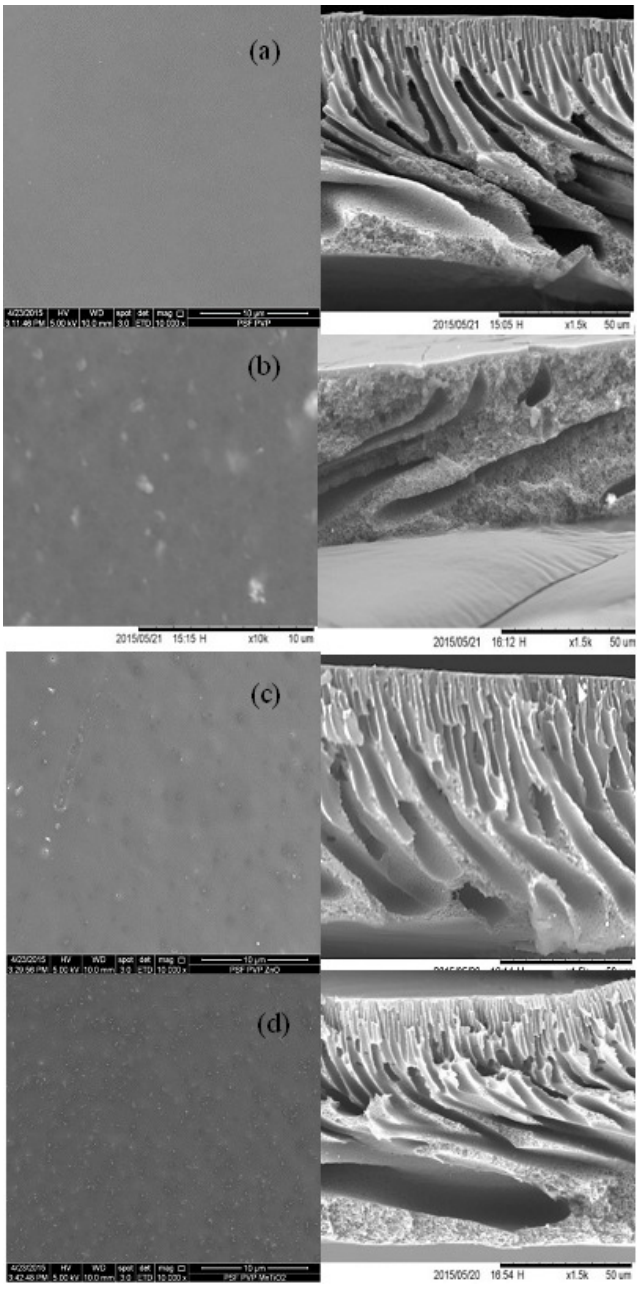

Fig. 1. SEM images of the surface (left) and cross section (right) of (a) PSf/PVP, (b) PSf/PVP/TiO_2, (c) PSf/PVP/ZnO and (d) PSf/PVP/Mn-TiO_2 membranes.

The PSf/PVP membrane showed a smooth surface without any defect. When different types of photocatalysts were added into the PSf/PVP membranes, asymmetric structures were observed in all these membranes. Serious agglomeration of particles was not found in the SEM images of PSf/PVP membranes with photocatalysts. The absence of agglomeration in this work could be related to the low loading of photocatalysts, as compared to the loading specified in other literature [30]. Furthermore, PVP helps in particle stabilization and prevents particle agglomeration as reported by others [31, 32]. The asymmetric structure of PSf/PVA, PSf/PVA/ZnO and PSf/PVA/ZnO-4 % membranes, is comprised of an ultrathin dense layer at the top and a sub-layer with macro voids at the bottom. The macro voids grew larger in PSf/PVA/ZnO membrane and they even grew into finger-like pores in the PSf/PVA/ZnO-4% membrane compared to the PSf/PVA membrane. The formation of finger-like pores depended on the permeability of the non-solvent into the membrane [33]. The addition of hydrophilic ZnO attracted more water for demixing and caused the nuclei to grow bigger during phase inversion, resulting in larger pores with good connectivity in the PSf/PVA/ZnO-4% membrane. The organic additive affected membrane morphology more significantly than the inorganic fillers. In addition, PVP was proven to be a better hydrophilic additive compared to PVA in the formation of finger-like pores for good separation performance.

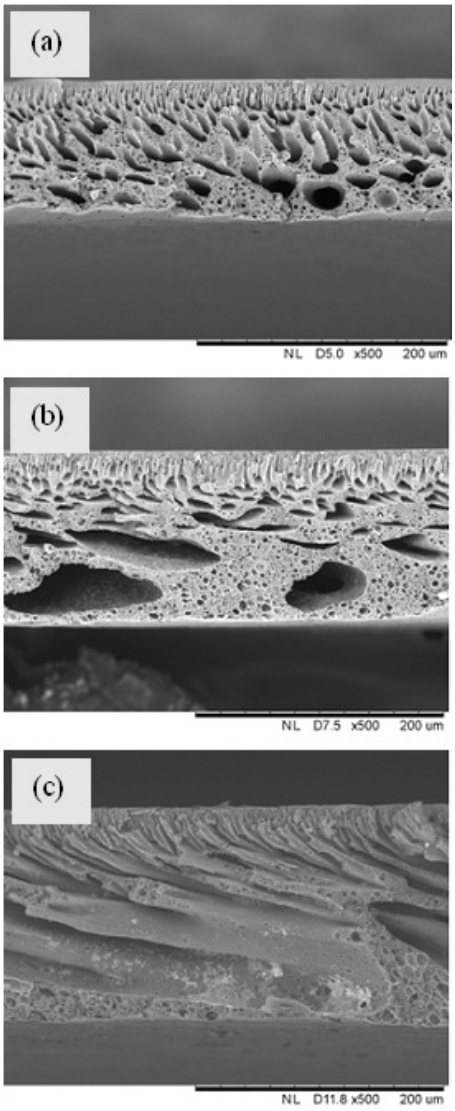

Fig. 2. SEM Images of the Cross Section (a) PSf/PVA, (b) PSf/PVA/ZnO, and (c) PSf/PVP/ZnO-4%.

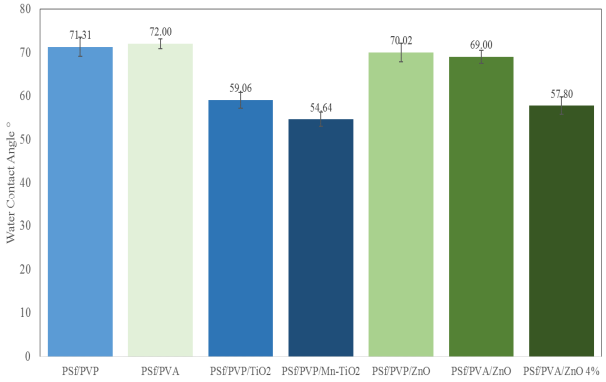

Fig. 3. Water contact angle on membrane samples.

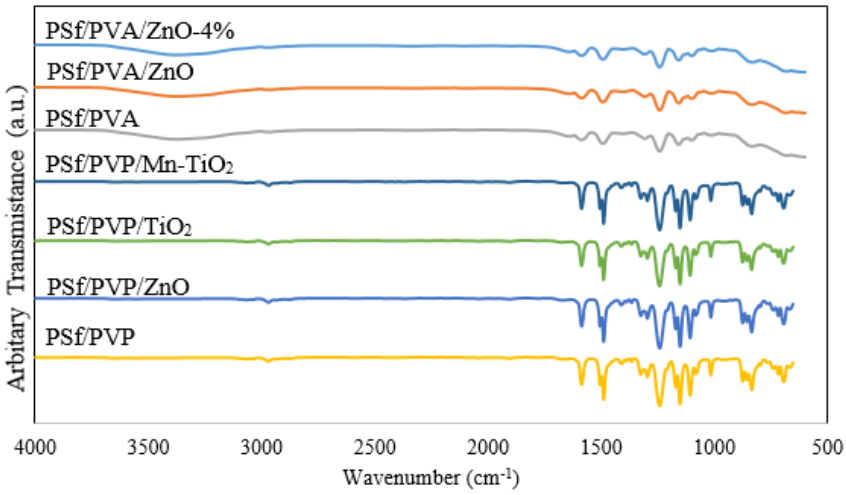

Fig. 4. FTIR patterns of the photocatalytic membranes.

Besides resulting in variations of membrane morphology, the addition of different photocatalysts also resulted in a variation of surface hydrophilicity as shown in Figure 3. The water contact angle on the PSf/PVP/TiO_2 membrane was 59.06 °, about 12 ° lower than that of the PSf/PVP membrane (71.31 °). This is because TiO_2 has high affinity towards water [34]. As expected, the Mn-doped TiO_2 nanoparticles caused a similar enhancement on membrane hydrophilicity because the doped nanoparticles consist of 99% TiO_2. Both PSf/PVA/ZnO and PSf/PVP/ZnO membranes only showed slight improvements in surface hydrophilicity, compared to the PSf/PVA membrane and PSf/PVP membrane, respectively. The surface hydrophilicity was improved only if a greater amount of ZnO nanoparticles were added into the PSf/PVA/ZnO-4% membrane. It was observed that ZnO nanoparticles settled faster than TiO_2 particles in the doped solution during the preparation of the membrane due to the density difference. Hence, it is reasonable to predict that less ZnO nanoparticles appeared on the surface of PSf/PVA/ZnO and PSf/PVP/ZnO membranes for the improvement of surface hydrophilicity compared to the PSf/PVA/TiO_2 membrane.

In addition, it is important to study the chemical changes on the membrane, due to the addition of additives and inorganic fillers. This is because the surface chemistry affects the separation performance of a membrane significantly. The functional groups of the PSf polymer contributed to the peaks at the specific wave number of 1150 cm^{-1} (symmetric O=S=O stretching), 1300 cm^{-1} (asymmetric O=S=O stretching), 1250 cm^{-1} (asymmetric C-O-C stretching), 1490 cm^{-1} and 1580 cm^{-1} (C=C aromatic ring stretching) as shown in Figure 4 [35]. The PSf membranes with PVP showed the additional peaks at 690 cm^{-1} and 2960 cm^{-1}, corresponding to amine stretching and asymmetric CH_2 ring stretching [36]. On the other hand, the distinct difference between the FTIR patterns of PSf/PVA membranes and the FTIR patterns of PSf/PVP membranes were the broadening of the peak from 3300 to 3500 cm^{-1}, which was caused by the vibration of the asymmetric hydroxyl group (-OH) from PVA [19]. However, the FTIR pattern of PSf/PVP membranes incorporated with different types of nanoparticles remained similar to the FTIR pattern of the PSf/PVP membrane without photocatalysts. The similarity could be related to the low concentration of nanoparticles that were added to these samples. The presence of photocatalysts in PSf membranes could only be confirmed using EDX (Figure 5). The element Zn appeared in the EDX result for the PSf/PVP/ZnO membrane while element Ti appeared in the EDX results for the PSf/PVP/TiO_2 and PSf/PVP/Mn-TiO_2 membranes. As mentioned earlier, since the amount of Mn in the doped TiO_2 is negligible, Mn was not detected in the EDX result for the PSf/PVP/Mn-TiO_2 membrane.

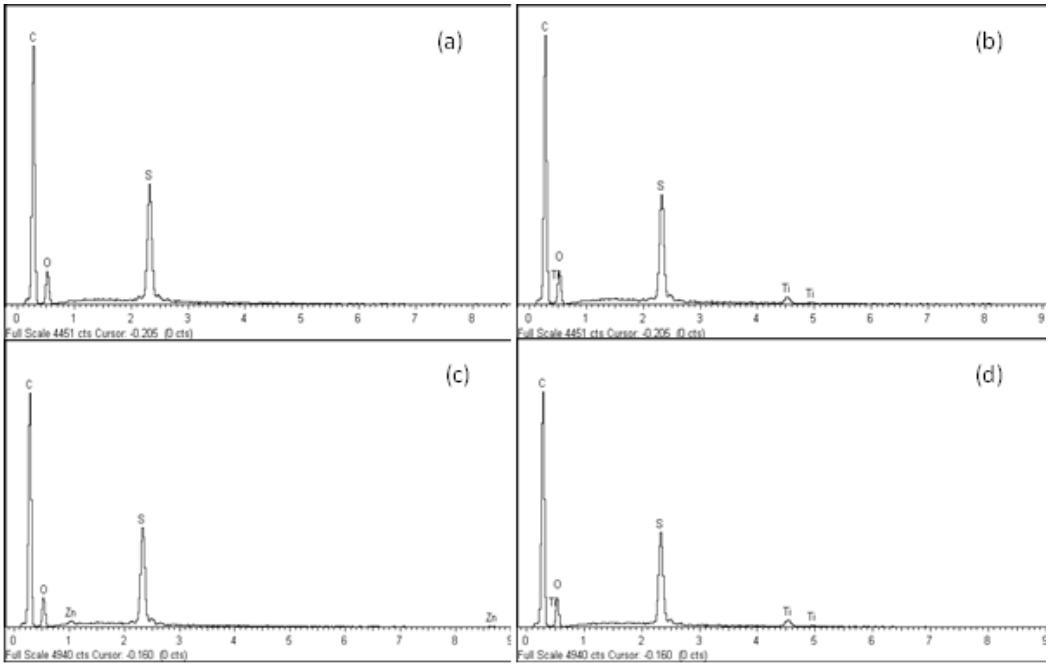

Fig. 5. EDX results of (a) PSf/PVP, (b) PSf/PVP/TiO_2, (c) PSf/PVP/ZnO and (d) PSf/PVP/Mn-TiO_2 membranes.

In addition, the major elements of PSf (C, S, and O) were successfully detected in all membrane samples as well. EDX results along the cross sectional lines of PSf/PVP/ZnO, PSf/PVA/ZnO and PSf/PVA/ZnO-4% membranes are presented in Figure 6. The good dispersion of ZnO in the PSf/PVP/ZnO membrane was confirmed because a low and uniform intensity of Zn was detected across this membrane. Large agglomerations of ZnO were expected to be absent in the PSf/PVP/ZnO membrane. With a similar ZnO loading, the PSf/PVA/ZnO membrane exhibited a very different EDX result compared to the PSf/PVP/ZnO membrane. Many peaks with a high intensity of the Zn element were observed in the EDX result of the PSf/PVA/ZnO membrane. These peaks were caused by agglomerates of fillers, as reported in our previous work [37]. A similar pattern was observed in the EDX result of the PSf/PVA/ZnO-4% membrane with higher ZnO content and more agglomeration. PVA was an inferior additive compared to PVP when it was used to disperse the nano–size photocatalysts.

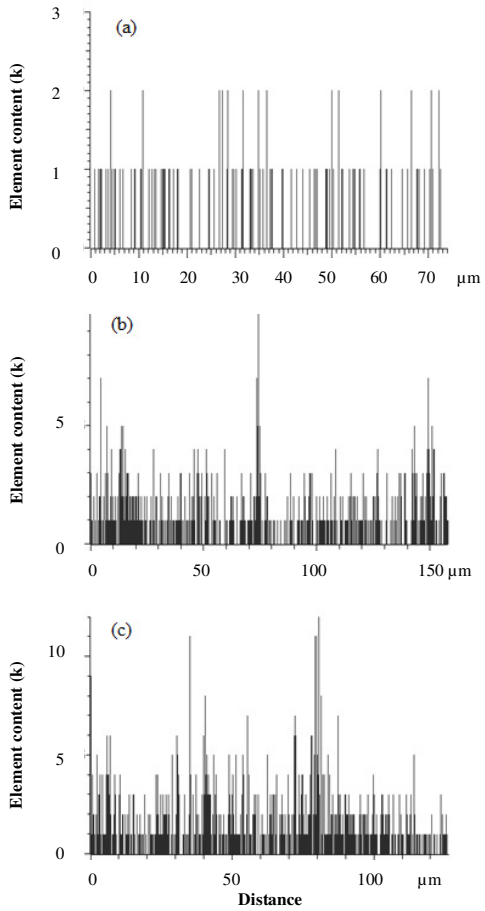

Fig. 6. EDX results showing Zn composition across cross sectional of (a) PSf/PVP/ZnO, (b) PSf/PVA/ZnO and (c) PSf/PVA/ZnO-4% membranes.

3.2. Changes in separation performance

Both PSf/PVA and PSf/PVP membranes exhibited a very low water permeability of 2.13 $L.m^{-2}.h^{-1}.bar^{-1}$ and 3.85 $L.m^{-2}.h^{-1}.bar^{-1}$, respectively. The incorporation of photocataysts (TiO_2, Mn-TiO_2 and ZnO) into the PSf membrane with PVP caused the water permeability to increase by six-to sevenfold as shown in Table 1. Increasing the ZnO loading in the PSf membrane with PVA resulted in permeability improvements as well. However, the improvement of the permeability of the PSf/PVA membrane incorporated with ZnO was less impressive. By adding more ZnO into the PSf/PVA membrane, the water permeability of the PSf/PVA/ZnO-4 % membrane increased slightly, up to 9.69 $L.m^{-2}.h^{-1}.bar^{-1}$. The improvement of membrane permeability could be related to the formation of finger-like pores and hydrophilic surfaces due to the addition of additives and photocatalysts.

Without the presence of photocatalysts, the PSf/PVP membrane showed a relatively low rejection of HA (31.15 %). The rejection of HA using PSf/PVP/Mn-TiO_2 and PSf/PVP/TiO_2 membranes only increased to 43.65 % and 49.92 % although these membranes showed great improvement of water permeability. The PSf/PVP/ZnO membrane on the other hand showed remarkable improvement of HA rejection, up to 71.76 %. Despite the additive difference, PSf/PVA/ZnO and PSf/PVA/ZnO-4 % membranes also showed astonishing HA rejection of 87.6 %. ZnO nanoparticles are preferable in the preparation of membranes for HA separation. A possible explanation is the formation of small pores for HA rejection after adding ZnO nanoparticles in PSf membranes.

Some of the recent researches have also shown the improvement of the membrane in water permeability and humic acid removal. De Sitter *et al.* [27] increased the membrane permeability approximately at threefold (20 $L.m^{-2}.h^{-1}.bar^{-1}$ to 63 $L.m^{-2}.h^{-1}.bar^{-1}$) by adding 30 wt.% of TiO_2. Hamid *et al.* [38] managed to improve the permeation of the hollow fiber membrane from 49.33 $L.m^{-2}.h^{-1}.bar^{-1}$ to 65.28 $L.m^{-2}.h^{-1}.bar^{-1}$ after adding 2 wt.% of TiO_2. However, none of them conducted the photocatalytic degradation test using the developed membranes. In this work, photocatalytic degradation tests were carried out to study the efficiency of photocatalysts after they were embedded in the membranes which will be discussed in the next section.

Table 1
Separation performance of photocatalytic membranes.

Membranes	Water Permeability ($L.m^{-2}.h^{-1}.bar^{-1}$)	Rejection of HA (%)
PSf/PVP	3.85	31.15
PSf/PVA	2.13	71.98
PSf/PVP/TiO_2	24.68	49.92
PSf/PVP/Mn-TiO_2	26.90	43.65
PSf/PVP/ZnO	23.22	71.76
PSf/PVA/ZnO	5.64	87.65
PSf/PVA/ZnO-4%	9.69	87.64

3.3. Changes in photo activity

Among the free photocatalytic nanoparticles, Mn-TiO_2 nanoparticles exhibited the best degradation of HA under UV radiation as summarized in Table 2. Mn-TiO_2 performed better than TiO_2 and ZnO because doping a photocatalyst with metals can narrow the band gap and lower the chances of recombining the exited electron with the holes [5].

Table 2
HA degradation using photocatalytic membrane.

Photocatalysts	HA degradation using free particles (%)	Membranes	HA degradation using particles in membrane (%)	Difference (%)
TiO_2	57.47	PSf/PVP/ TiO_2	42.89	14.58
Mn-TiO_2	63.35	PSf/PVP-Mn-TiO_2	54.28	9.07
ZnO (2%)	53.48;	PSf/PVP/ZnO	48.07	5.41
	50.68	PSf/PVA/ZnO	13.26;	37.42
ZnO (4%)	85.80	PSf/PVA/ZnO-4%	3.46	82.34

Inevitably, the photocatalytic hindrance was expected after incorporating the photocatalysts into the polymeric matrix. The hindrance was due to the limited transmittance of light and the restricted contact with the contaminant in the polymeric matrix. However, such hindrance could be reduced by developing suitable membrane morphology. The PSf/PVP/ZnO membrane performed immensely better than the PSf/PVA/ZnO membrane in the photo degradation of HA, although the amount of photocatalysts in these membranes was the same. The better performance of the PSf/PVP/ZnO membrane in photocatalytic degradation might be due to the existence of finger-like structures for HA penetration and the good dispersion of photocatalysts. The extremely poor performance of the PSf/PVP/ZnO-4 % membrane under UV light may be due to the serious agglomeration of ZnO nanoparticles in the polymeric matrix as reported in the literatures [16].

4. Conclusion

Organic additives and photocatalysts play an important role in the development of photocatalytic membranes as they contribute to morphological, hydrophilic and chemical changes in membranes. The formation of finger-like pores was greatly promoted by PVP and slightly enhanced by photocatalyst loading. The hindrance of photo activity could be reduced in the presence of these finger-like pores. The contact between HA and the photocatalyst was less hindered in the polymeric matrix with finger-like pores. ZnO nanoparticles were suitable in the development of membranes for HA separation because a high rejection of HA was recorded independently of the selection of organic additives.

5. Acknowledgements

The authors acknowledge financial support from Universiti Sains Malaysia (Membrane Science and Technology Cluster), Ministry of Education Malaysia (FRGS/2/2013/TK05/USM/02/5) and MyBrain15.

6. References

[1] N. Muhd Julkapli, S. Bagheri, S. Bee Abd Hamid, Recent advances in heterogeneous photocatalytic decolorization of synthetic dyes, Scientific World J., 2014 (2014) 1-25.

[2] P. Jiang, D. Ren, D. He, W. Fu, J. Wang, M. Gu, An easily sedimentable and effective TiO_2 photocatalyst for removal of dyes in water, Sep. Purif. Technol. 122 (2014) 128-132.

[3] H. Choi, E. Stathatos, D.D. Dionysiou, Photocatalytic TiO_2 films and membranes for the development of efficient wastewater treatment and reuse systems, Desalination 202 (2007) 199-206.

[4] Y. Wang, Y. Huang, W. Ho, L. Zhang, Z. Zou, S. Lee, Biomolecule-controlled hydrothermal synthesis of C–N–S-tridoped TiO_2 nanocrystalline photocatalysts for NO removal under simulated solar light irradiation, J. Hazard. Mater. 169 (2009) 77-87.

[5] L. Wang, X. Zhang, P. Zhang, Z. Cao, J. Hu, Photoelectric conversion performances of Mn doped TiO_2 under > 420nm visible light irradiation, J. Soudi Chem. Soc. 19 (2015) 595-601.

[6] P. Chandran, S. Netha, S.S. Khan, Effect of humic acid on photocatalytic activity of ZnO nanoparticles, J. Photochem. Photobiol. B 138 (2014) 155-159.

[7] M. Nirmala, M.G. Nair, K. Rekha, A. Anukaliani, S. Samdarshi, R.G. Nair, Photocatalytic activity of ZnO nanopowders synthesized by DC thermal plasma, Afr. J. Basic Appl. Sci. 2 (2010) 161-166.

[8] S. Kuriakose, V. Choudhary, B. Satpati, S. Mohapatra, Enhanced photocatalytic activity of Ag–ZnO hybrid plasmonic nanostructures prepared by a facile wet chemical method, Beilstein J. Nanotechnol. 5 (2014) 639-650.

[9] J. Kim, A. Sotto, J. Chang, D. Nam, A. Boromand, B. Van der Bruggen, Embedding TiO_2 nanoparticles versus surface coating by layer-by-layer deposition on nanoporous polymeric films, Microp. Mesop. Mater. 173 (2013) 121-128.

[10] S. Liang, K. Xiao, Y. Mo, X. Huang, A novel ZnO nanoparticle blended polyvinylidene fluoride membrane for anti-irreversible fouling, J. Membr. Sci. 394 (2012) 184-192.

[11] H. Rajabi, N. Ghaemi, S.S. Madaeni, P. Daraei, B. Astinchap, S. Zinadini, S.H. Razavizadeh, Nano-ZnO embedded mixed matrix polyethersulfone (PES) membrane: influence of nanofiller shape on characterization and fouling resistance, Appl. Surf. Sci. 349 (2015) 66-77.

[12] T.-H. Bae, T.-M. Tak, Effect of TiO_2 nanoparticles on fouling mitigation of ultrafiltration membranes for activated sludge filtration, J. Membr. Sci. 249 (2005) 1-8.

[13] T.H. Bae, T.M. Tak, Preparation of TiO_2 self-assembled polymeric nanocomposite membranes and examination of their fouling mitigation effects in a membrane bioreactor system, J. Membr. Sci. 266 (2005) 1-5.

[14] T.H. Bae, I.C. Kim, T.M. Tak, Preparation and characterization of fouling-resistant TiO_2 self-assembled nanocomposite membranes, J. Membr. Sci. 275 (2006) 1-5.

[15] H. Song, J. Shao, J. Wang, X. Zhong, The removal of natural organic matter with LiCl–TiO_2-doped PVDF membranes by integration of ultrafiltration with photocatalysis, Desalination 344 (2014) 412-421.

[16] C.P. Leo, W.C. Lee, A.L. Ahmad, A.W. Mohammad, Polysulfone membranes blended with ZnO nanoparticles for reducing fouling by oleic acid, Sep. Purif. Technol. 89 (2012) 51-56.

[17] G. Dong, H. Li, V. Chen, Challenges and opportunities for mixed-matrix membranes for gas separation, J. Mater. Chem. A 1 (2013) 4610-4630.

[18] S.H. Othman, S.A. Rashid, T.I.M. Ghazi, N. Abdullah, Dispersion and stabilization of photocatalytic TiO_2 nanoparticles in aqueous suspension for coatings applications, J. Nanomater. 2012 (2012) 2.

[19] B. Rajaeian, A. Heitz, M.O. Tade, S. Liu, Improved separation and antifouling performance of PVA thin film nanocomposite membranes incorporated with carboxylated TiO_2 nanoparticles, J. Membr. Sci. 485 (2015) 48-59.

[20] B. Faure, G. Salazar-Alvarez, A. Ahniyaz, I. Villaluenga, G. Berriozabal, Y.R. De Miguel, L. Bergström, Dispersion and surface functionalization of oxide nanoparticles for transparent photocatalytic and UV-protecting coatings and sunscreens, Sci. Technol. Adv. Mater. 14 (2013) 1-23.

[21] M.H. Nia, M. Rezaei-Tavirani, A.R. Nikoofar, H. Masoumi, R. Nasr, H. Hasanzadeh, M. Jadidi, M. Shadnush, Stabilizing and dispersing methods of TiO_2 nanoparticles in biological studies, J. Paramed. Sci. 6 (2015).

[22] J.K. Pi, H.C. Yang, L.S. Wan, J. Wu, Z.-K. Xu, Polypropylene microfiltration membranes modified with TiO_2 nanoparticles for surface wettability and antifouling property, J. Membr. Sci. 500 (2015) 8-15.

[23] H. Bai, X. Zan, L. Zhang, D.D. Sun, Multi-functional CNT/ZnO/TiO_2 nanocomposite membrane for concurrent filtration and photocatalytic degradation, Sep. Purif. Technol. 156 (2015) 922-930.

[24] I. Wienk, R. Boom, M. Beerlage, A. Bulte, C. Smolders, H. Strathmann, Recent advances in the formation of phase inversion membranes made from amorphous or semi-crystalline polymers, J. Membr. Sci. 113 (1996) 361-371.

[25] R. Boom, I. Wienk, T. Van den Boomgaard, C. Smolders, Microstructures in phase inversion membranes. part 2. the role of a polymeric additive, J. Membr. Sci. 73 (1992) 277-292.

[26] A. Ahmad, N. Ideris, B. Ooi, S. Low, A. Ismail, Morphology and polymorph study of a polyvinylidene Fluoride (PVDF) membrane for protein binding: effect of the dissolving temperature, Desalination 278 (2011) 318-324.

[27] K. De Sitter, C. Dotremont, I. Genné, L. Stoops, The use of nanoparticles as alternative pore former for the production of more sustainable polyethersulfone ultrafiltration membranes, J. Membr. Sci. 471 (2014) 168-178.

[28] H. Matsuyama, T. Maki, M. Teramoto, K. Kobayashi, Effect of PVP additive on porous polysulfone membrane formation by immersion precipitation method, Sep. Sci. Technol. 38 (2003) 3449-3458.

[29] E. Saljoughi, M. Amirilargani, T. Mohammadi, Effect of Poly(vinyl pyrrolidone) concentration and coagulation bath temperature on the morphology, permeability, and thermal stability of asymmetric cellulose acetate membranes, J. Appl. Polym. Sci. 111 (2009) 2537-2544.

[30] Y. Yang, H. Zhang, P. Wang, Q. Zheng, J. Li, The influence of nano-sized TiO_2 fillers on the morphologies and properties of PSF UF membrane, J. Membr. Sci. 288 (2007) 231-238.

[31] S. Zhao, Z. Wang, X. Wei, X. Tian, J. Wang, S. Yang, S. Wang, Comparison study of the effect of PVP and PANI nanofibers additives on membrane formation mechanism, structure and serformance, J. Membr. Sci. 385 (2011) 110-122.

[32] H. Basri, A.F. Ismail, M. Aziz, Polyethersulfone (PES)–silver composite UF membrane: effect of silver loading and PVP molecular weight on membrane morphology and antibacterial activity, Desalination 273 (2011) 72-80.

[33] T.H. Young, L.W. Chen, Pore formation mechanism of membranes from phase inversion process, Desalination 103 (1995) 233-247.

[34] M. Jyothi, V. Nayak, M. Padaki, R.G. Balakrishna, A. Ismail, The effect of UV irradiation on PSf/TiO_2 mixed matrix membrane for chromium rejection, Desalination 354 (2014) 189-199.

[35] D. Emadzadeh, W. Lau, T. Matsuura, M. Rahbari-Sisakht, A. Ismail, A novel thin film composite forward osmosis membrane prepared from PSf–TiO_2 nanocomposite substrate for water desalination, Chem. Eng. J. 237 (2014) 70-80.

[36] Y. Borodko, S.E. Habas, M. Koebel, P. Yang, H. Frei, G.A. Somorjai, Probing the interaction of poly(vinylpyrrolidone) with platinum nanocrystals by UV-Raman and FTIR, J. Phys. Chem. B 110 (2006) 23052-23059.

[37] M. Junaidi, C. Khoo, C. Leo, A. Ahmad, The effects of solvents on the modification of SAPO-34 zeolite using 3-aminopropyl trimethoxy silane for the preparation of asymmetric polysulfone mixed matrix membrane in the application of CO_2 separation, Microp. Mesop. Mater. 192 (2014) 52-59.

[38] N. Hamid, A.F. Ismail, T. Matsuura, A. Zularisam, W.J. Lau, E. Yuliwati, M.S. Abdullah, Morphological and separation performance study of polysulfone/titanium dioxide (PSF/TiO_2) ultrafiltration membranes for humic acid removal, Desalination 273 (2011) 85-92.